Identification of a developmentally regulated pathway of membrane retrieval in neuronal growth cones

Dario Bonanomi[1,*,‡], Eugenio F. Fornasiero[1,*], Gregorio Valdez[2,§], Simon Halegoua[2], Fabio Benfenati[3,4,5], Andrea Menegon[1] and Flavia Valtorta[1,5,¶]

[1]S. Raffaele Scientific Institute/Vita-Salute University and IIT Unit of Molecular Neuroscience, 20132 Milano, Italy
[2]Department of Neurobiology and Behavior, State University of New York at Stony Brook, Stony Brook, NY 11794, USA
[3]Department of Experimental Medicine, University of Genova, 16132 Genova, Italy
[4]Department of Neuroscience and Brain Technologies, IIT Central Laboratories, 16163 Genova, Italy
[5]Istituto Nazionale di Neuroscienze, 10125 Torino, Italy

*These authors contributed equally to this work
‡Present address: Gene Expression Laboratory, The Salk Institute for Biological Studies, La Jolla, CA 92037, USA
§Present address: Department of Molecular and Cellular Biology, Harvard University, Cambridge, MA 02138, USA
¶Author for correspondence (e-mail: valtorta.flavia@hsr.it)

Accepted 12 August 2008
Journal of Cell Science 121, 3757-3769 Published by The Company of Biologists 2008
doi:10.1242/jcs.033803

Summary

The growth-cone plasma membrane constantly reconfigures during axon navigation and upon target recognition. The identity and regulation of the membrane pathway(s) participating in remodeling of the growth-cone surface remain elusive. Here, we identify a constitutive, high-capacity plasma-membrane-recycling activity in the axonal growth cones, which is mediated by a novel bulk endocytic pathway that is mechanistically related to macropinocytosis. This pathway generates large compartments at sites of intense actin-based membrane ruffling through the actions of phosphatidylinositol 3-kinase, the small GTPase Rac1 and the pinocytic chaperone Pincher. At early developmental stages, bulk endocytosis is the primary endocytic pathway for rapid retrieval of the growth-cone plasma membrane. At later stages, during the onset of synaptogenesis, an intrinsic program of maturation leads to downregulation of basal bulk endocytosis and the emergence of depolarization-induced synaptic-vesicle exo-endocytosis. We propose that the control of bulk membrane retrieval contributes to the homeostatic regulation of the axonal plasma membrane and to growth-cone remodeling during axonal outgrowth. In addition, we suggest that the downregulation of bulk endocytosis during synaptogenesis might contribute to the preservation of synaptic-vesicle specificity.

Supplementary material available online at
http://jcs.biologists.org/cgi/content/full/121/22/3757/DC1

Key words: Endocytosis, Axolemma, Synaptic vesicle, Trafficking, Fluorescence microscopy

Introduction

In the nervous system, axons are guided to their specific targets by highly motile growth cones, present at their distal tip, which exhibit a remarkable organization. Operationally, they include a peripheral (P) domain composed of actin-rich lamellipodia and filopodia, a central (C) domain containing microtubules and various organelles, and a transitional (T) domain located at the interface between the P and C domains, characterized by intense F-actin remodeling and membrane ruffling (Dailey and Bridgman, 1989; Forscher and Smith, 1988; Schaefer et al., 2002). During axon navigation and synapse formation, growth cones respond to environmental cues with drastic rearrangements of their membrane and cytoskeletal components (Dent and Gertler, 2003).

The growth cone is recognized as the major site of axonal membrane addition and recycling (Bray, 1970; Sinclair et al., 1988; Parton et al., 1992; Craig et al., 1995; Zakharenko and Popov, 2000); however, the control of its membrane dynamics during axon growth and retraction is still poorly understood. Earlier ultrastructural analyses reported the localization of a plethora of organelles, still largely undefined in terms of identity, in the C domain (Yamada et al., 1971; Pfenninger and Maylié-Pfenninger, 1981; Tsui et al., 1983; Cheng and Reese, 1985). Some of these organelles, including clusters of synaptic vesicle (SV) precursors (Fletcher et al., 1991), are exocytic and are subjected to regulatory mechanisms similar to those operative at mature synapses (Bonanomi et al., 2005). These precursors contribute to the formation of the presynaptic pool of vesicles at nascent synaptic contacts (Chow and Poo, 1985; Matteoli et al., 1992; Ahmari et al., 2000) (for a review, see Bonanomi et al., 2006) but have no role in neurite outgrowth or in the expansion of the growth-cone plasma membrane (Lockerbie et al., 1991; Leoni et al., 1999; Verhage et al., 2000).

Endocytosis in the growth cone has been shown to take place by at least two processes, one constitutive and one evoked, carried out by distinct populations of vesicles (Diefenbach et al., 1999). Interestingly, these processes do not operate independently, but function coordinately with exocytosis and in strict interaction with cytoskeletal dynamics. As a consequence, endocytosis is enhanced during growth-cone collapse that is induced by repulsive cues (Fournier et al., 2000; Jurney et al., 2002), but is also required for axon outgrowth (Kim and Wu, 1987; Torre et al., 1994; Mundigl et al., 1998; Albertinazzi et al., 2003). Counterintuitively, membrane retrieval at the newly formed growth cone is a main process associated with vigorous extension of axons after axotomy (Ashery et al., 1996). Rapid, bidirectional changes of surface membrane do therefore take place at growth cones during axon navigation. By combining imaging of endocytic tracers with interference and overexpression approaches, we investigated the nature and properties of the endocytic processes taking place at the growth cones of developing hippocampal neurons in culture.

Results

Bulk endocytosis at the axonal growth cone

To study constitutive membrane recycling in the growth cone, we used rat hippocampal neurons at 2-3 days in vitro (DIV) (stage 3) (Dotti et al., 1988) displaying an unequivocally identifiable axon tipped with a growth cone. Neurons incubated in basal medium [Krebs-Ringer-HEPES (KRH)] were exposed to the styryl dye FM4-64, which binds reversibly to the outer surface of the plasma membrane and is internalized in endocytic vesicles (Betz and Bewick, 1992; Betz et al., 1996) (Fig. 1A). After a brief (1 minute) incubation, intense fluorescence appeared in 59±16% (mean ± s.e.m.) of growth cones; this fluorescence was associated with large structures, often exhibiting a vacuolar organization, that were clustered at the distal edge of the C domain. By contrast, FM4-64 staining was undetectable in both the lamellar P domain of the growth cone and the axon shaft. The axonal specificity of this bulk endocytosis was confirmed by retrospective staining of the neurons for the marker dephospho-Tau1 (Fig. 1B).

Interestingly, at each axonal branching, bulk endocytic accumulation of the dye was typically maintained in only one of the growth cones (Fig. 1C). The presence or absence of bulk endocytic activity was unrelated to the growth-cone area (Fig. 2B), but it was positively correlated with the growth-cone mobility, as revealed by time-lapse imaging followed by FM4-64 loading (Fig. 2A,C; supplementary material Movies 1 and 2).

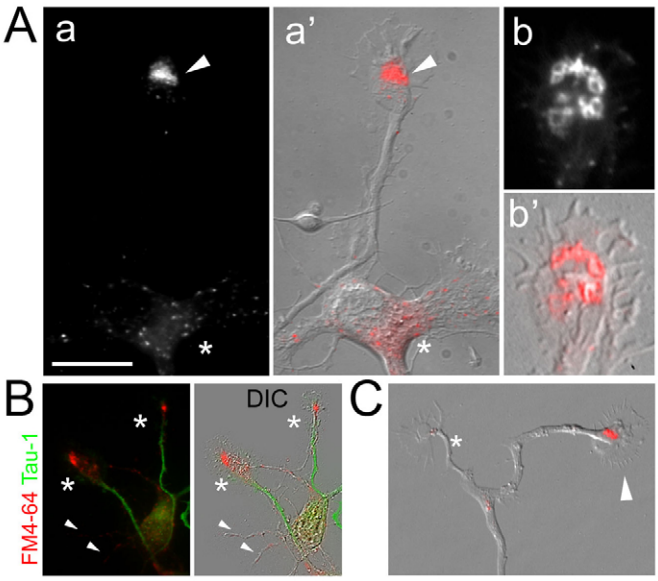

Fig. 1. Constitutive bulk membrane retrieval in axonal growth cones. (A) Basal uptake of FM4-64 (red in a′ and b′) in neurons at 2 DIV that were incubated with KRH containing the dye and imaged after a 2-minute washing. (a,a′) A broad region of intense FM4-64 staining is associated with the growth cone (arrowhead), whereas few dispersed punctae appear in the cell body (asterisk). Note the lack of FM4-64 internalization along the axon shaft. (b,b′) Higher-magnification views of a growth cone, showing internalization of FM4-64 in large organelles at the interface between the central and peripheral domains (T domain). Note the vacuolar organization of the FM4-64-positive compartment in b. (B) Basal uptake of FM4-64 (red) in neurons incubated with the dye for 1 minute, fixed and retrospectively stained for the axon-specific marker dephospho-Tau-1 (green). Intense FM4-64 uptake is visible in growth cones of Tau-1-positive axons (asterisks) but not in Tau-1-negative perspective dendrites (arrowheads). (C) Differential uptake of FM4-64 (red) in growth cones that are associated with distinct axonal branches of the same neuron. One of the growth cones (arrowhead) shows strong constitutive endocytosis, whereas the other (asterisk) is inactive. Scale bar: 13.5 μm (Aa,a′); 5 μm (Ab,b′); 25 μm (B); 10 μm (C).

Bulk endocytosis might be driven by the rapid addition of Golgi-derived membrane to the growth cone. Alternatively, signaling events within the growth cone might recruit bulk endocytosis to allow for rapid local changes. To distinguish between these two possibilities, we exposed neurons to various treatments. Constitutive FM4-64 uptake was prevented by incubation of neurons at 4°C, a treatment that attenuates endocytic processes. By contrast, bulk endocytosis was not affected by prolonged (30 minute) incubation of neurons in Ca^{2+}-free KRH, a maneuver leading to depletion of intracellular Ca^{2+} stores (Cohen and Fields, 2006), or by a 1-hour incubation in the presence of BFA, an ADP-ribosylation factor-1 inhibitor that prevents traffic from the Golgi complex (Lippincott-Schwartz et al., 1989; Miller et al., 1992) and blocks axon growth (Jareb and Banker, 1997) (Fig. 3A,C).

To determine the intracellular fate of bulk endosomes, we visualized the movement of internalized FM4-64. We found that internalized FM4-64 is progressively released during a 30-minute washing (Fig. 3C; Fig. 6). We also observed organelles containing FM4-64 moving retrogradely along the axon (supplementary material Fig. S1). These results suggest that bulk endocytosis leads to the generation of recycling vesicles and vesicles that take cargo to the cell body.

Bulk endocytosis shares several features with macropinocytosis

Time-lapse differential interference contrast (DIC) imaging of growth cones of stage-3 neurons exposed to FM4-64 in KRH for 1 minute revealed a tight correlation between the sites of bulk constitutive endocytosis and the sites of plasma-membrane ruffling, which is particularly intense in the T domain (see also Forscher et al., 1992; Schaefer et al., 2002) (Fig. 3B). In the T zone, the compartments of bulk FM4-64 uptake overlapped with F-actin-rich ruffling hotspots (Fig. 3D). F-actin disruption by cytochalasin D, which impairs the addition of actin monomers to filaments, significantly reduced basal FM4-64 uptake, indicating that actin polymerization is required for constitutive plasma-membrane retrieval in the growth cone (Fig. 3A,C).

Phosphatidylinositol 3-kinase (PI3-kinase) is localized at the tip of newly specified axons of stage-3 neurons (Shi et al., 2003). In other cell types, this enzyme has been implicated in high-volume endocytosis (Lindmo and Stenmark, 2006). Application of the selective PI3-kinase inhibitor LY294002 significantly reduced constitutive FM4-64 uptake (Fig. 3A,C).

Staining of neurons with filipin, a fluorescent marker of cholesterol, revealed an enrichment of this lipid in the C domain, partially overlapping with the compartments of bulk FM4-64 internalization (Fig. 3E). Acute (3 minutes) cholesterol extraction with methyl-β-cyclodextrin (MβCD) drastically affected FM4-64 uptake in the growth cones (Fig. 3A,C).

To confirm that the vacuolar compartments emanated from bulk endocytosis and not from the fusion of small vesicles, we carried out additional experiments using macropinocytic markers (Reece et al., 2001; Falcone et al., 2006). Again, we observed intense bulk endocytosis in the C domain, by using the membrane-impermeable fluid-phase fluorescent dye Lucifer yellow or green fluorescent polystyrene beads (20 nm in diameter). A similar pattern of endocytosis was visible after exposure to large fluid-phase markers, either fluorescent beads (200 nm in diameter) or 40-kDa dextran, which have restricted access to small vesicles (Fig. 4B and data not

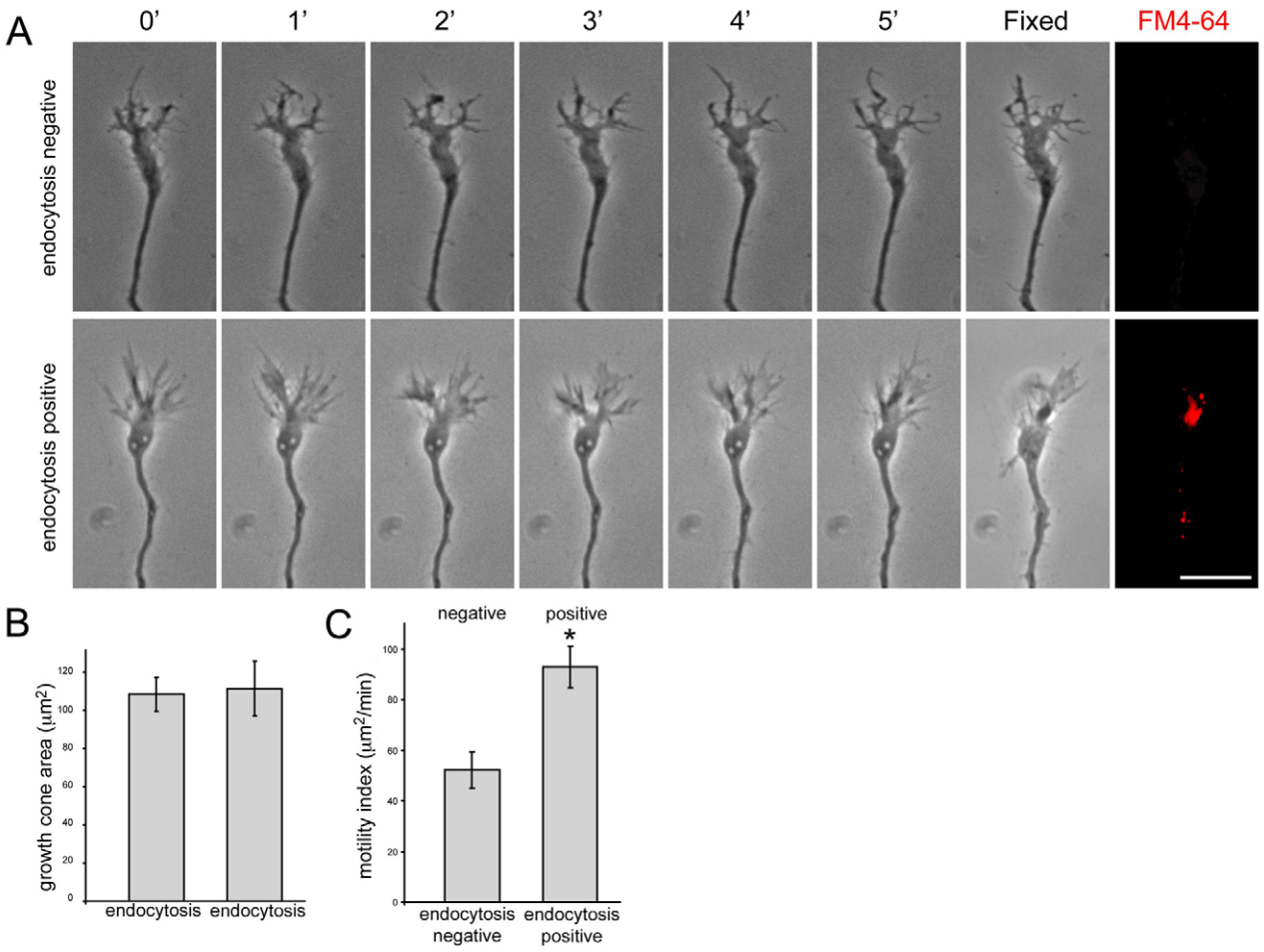

Fig. 2. Bulk endocytosis correlates with growth-cone motility. (A) Time-lapse phase-contrast imaging of two representative growth cones (3 DIV) over a 5-minute period prior to exposure to FM4-64 for 1 minute and fixation. The dye is internalized only in the more motile growth cone (bottom panels). (B) Quantification of the area of growth cones that are either positive or negative for bulk FM4-64 endocytosis (mean ± s.e.m.; n>70 growth cones per condition). (C) Quantification of growth-cone motility in growth cones that are either positive or negative for bulk FM4-64 endocytosis. The motility index (μm^2/minute) was calculated by measuring the variation in growth-cone area over the course of 6 minutes as described in the Materials and Methods (mean ± s.e.m.; n=25 growth cones from three independent preparations; *P<0.01, Student's t test, endocytosis-positive vs endocytosis-negative growth cones). Bulk endocytosis is preferentially associated with more-dynamic growth cones. Scale bar: 5 μm.

shown). Moreover, in growth cones labeled with the 20-nm beads and subsequently exposed to FM4-64, the two tracers displayed largely overlapping patterns of internalization (Fig. 4B). As observed for FM4-64 uptake, the constitutive internalization of 20-nm beads was inhibited by F-actin disruption, PI3-kinase inhibition and cholesterol depletion. Bead uptake was recovered 30 minutes after MβCD washout, in parallel to the normalization of cholesterol levels (supplementary material Fig. S2).

Finally, we probed the localization of FM4-64 with Rabankyrin-5, a Rab5 effector that modulates macropinocytosis in non-neuronal cells (Schnatwinkel et al., 2004). Interestingly, FM4-64 and Rabankyrin-5 were found partially colocalized at the growth cone (Fig. 4E). Our findings indicate that, at early developmental stages, a rapid constitutive process of bulk plasma-membrane internalization is associated with highly motile axonal growth cones and shows features of a macropinocytosis-related pathway.

Bulk endocytosis functions independently of clathrin

The C domain of the growth cone is characterized by a high density of organelles, including endosomes and SVs. In order to investigate the possible involvement of these vesicles in bulk endocytosis, we carried out retrospective staining of FM4-64-loaded growth cones with the SV marker synaptobrevin-2 [also known as vesicle-associated membrane protein 2 (VAMP2)] or the endosomal marker syntaxin 13. In both cases, virtually no colocalization with the compartments of constitutive plasma-membrane uptake was observed (Fig. 4A).

The fast, efficient uptake of 200-nm-diameter beads and the lack of colocalization with clathrin-derived vesicles were suggestive of a clathrin-independent endocytic pathway (Rejman et al., 2004). Along this line, Alexa-Fluor-488-conjugated transferrin, a marker of clathrin-mediated endocytosis, was internalized into endosomes in the cell body but not in the compartments of bulk FM4-64 uptake in the growth cone (Fig. 4D). To more directly test a role for clathrin in bulk endocytosis, we knocked down the clathrin heavy chain (CHC) using short interfering RNA (RNAi) (Lampugnani et al., 2006; Granseth et al., 2006) in cells that were later probed for FM4-64 uptake (Fig. 4C). Effective downregulation of CHC, as assessed by retrospective immunofluorescence of growth cones, did not affect

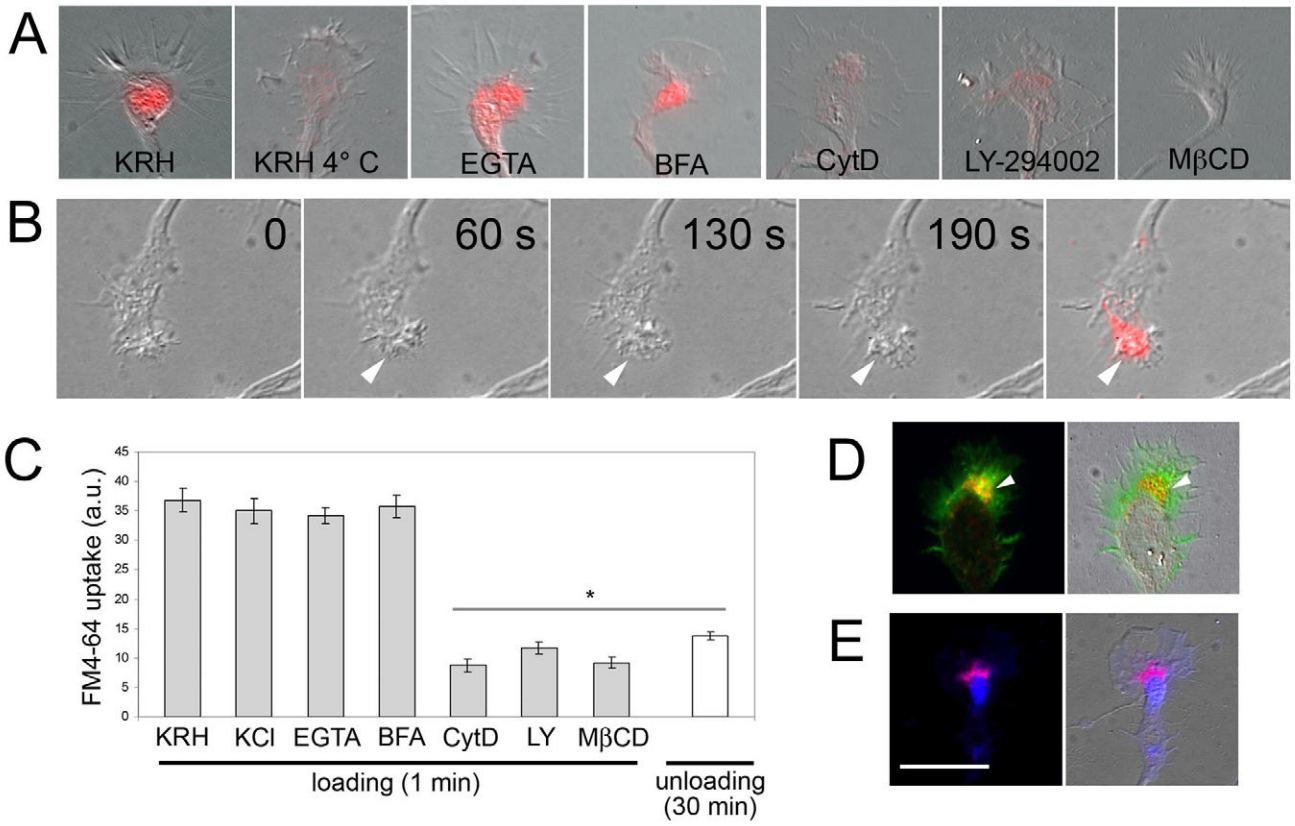

Fig. 3. Bulk endocytosis in the growth cone is linked to membrane ruffling and depends on actin dynamics, PI3-kinase activity and cholesterol levels. (A) Growth cones (2 DIV) that were either left untreated (KRH) or subjected to various treatments before incubation for 1 minute with KRH in the presence of FM4-64 are shown. Incubation of growth cones at 4°C during FM4-64 application prevents dye uptake (KRH 4°C). Incubation with either 2 mM EGTA-containing solution devoid of Ca^{2+} for 30 minutes (EGTA) or BFA (10 μg/ml) for 1 hour does not affect FM4-64 internalization. Treatments with CytD (10 μM, 15 minutes), LY294002 (50 μm, 30 minutes) or MβCD (5 mM, 3 minutes) inhibit FM4-64 uptake. (B) Time-lapse DIC imaging of a growth cone (2 DIV) incubated for 130 seconds in KRH prior to exposure for 1 minute to KRH containing FM4-64. The last panel on the right represents the overlay of the DIC image taken at 190 seconds with the FM4-64 staining (red). The dye is internalized in the region of the growth cone that is associated with active plasma-membrane ruffling (arrowhead). (C) Quantification of FM4-64 uptake in growth cones that were treated as shown in A. The amounts of FM4-64 loaded in 2-DIV growth cones during a 1-minute incubation in high K^+ (KCl) or remaining after incubation in KRH for 30 minutes at 37°C (unloading) are also reported (mean ± s.e.m.; *n*=30-40 growth cones per treatment; **P*<0.001, Dunnett's test for untreated growth cones vs growth cones subjected to various treatments). (D,E) Growth cones loaded with FM4-64 (KRH, 1 minute; red) and retrospectively stained with either FITC-phalloidin to visualize F-actin (D; green) or filipin to visualize cholesterol (E; blue). The overlay between the corresponding fluorescence and DIC images is shown in the right panels. The arrowhead in D points to a ruffling focus colocalizing with FM4-64 labeling. Scale bar: 10 μm.

FM4-64 uptake, indicating that the bulk plasma-membrane retrieval was indeed clathrin-independent.

Selectivity of bulk endocytosis

We investigated whether, at the growth cone, bulk endocytosis mediated selective internalization of plasma-membrane proteins that were internalized via other endocytic pathways. Growth cones were loaded with FM4-64 during a 1-minute-incubation in resting solution, immediately fixed and retrospectively stained for Trk, L1, β1 integrin or APP, four proteins that undergo recycling at the axonal plasma membrane (Yamazaki et al., 1995; Condic and Letourneau, 1997; Kamiguchi and Lemmon, 2000; Chen et al., 2005) (Fig. 5). None of these membrane proteins colocalized with the FM4-64-positive compartments.

Next, we monitored over time the internalization of FM4-64 applied to the same growth cone together with another marker, Alexa-Fluor-488-conjugated cholera toxin B subunit (CtxB), which binds the lipid-raft component ganglioside GM1 (Fig. 6). In other cell types, CtxB is internalized via clathrin-coated pits, caveolae (Torgersen et al., 2001) or clathrin-independent pathways (Kirkham et al., 2005). After a 1-minute-incubation, when FM4-64 was already internalized in large compartments at the T domain of the growth cone, CtxB was still associated with the plasma membrane. During the following 30 minutes, fluorescent CtxB was redistributed into puncta, most probably corresponding to endocytic vesicles enriched at the T domain. At no time point did the pattern of CtxB overlap with the FM4-64-positive compartments. These results reveal the exclusivity of bulk endocytosis and document the existence, at the growth cone, of one (or more) sorting processes that exclude most specific plasma-membrane components from the bulk endocytic organelles.

Rac1 controls bulk plasma-membrane retrieval in the growth cone

Rac1 has been implicated in the stimulation of membrane ruffling and bulk fluid-phase uptake (i.e. macropinocytosis) in non-neuronal cells (Symons and Rusk, 2003). Thus, we reasoned that Rac1 might participate in the process of constitutive plasma-membrane

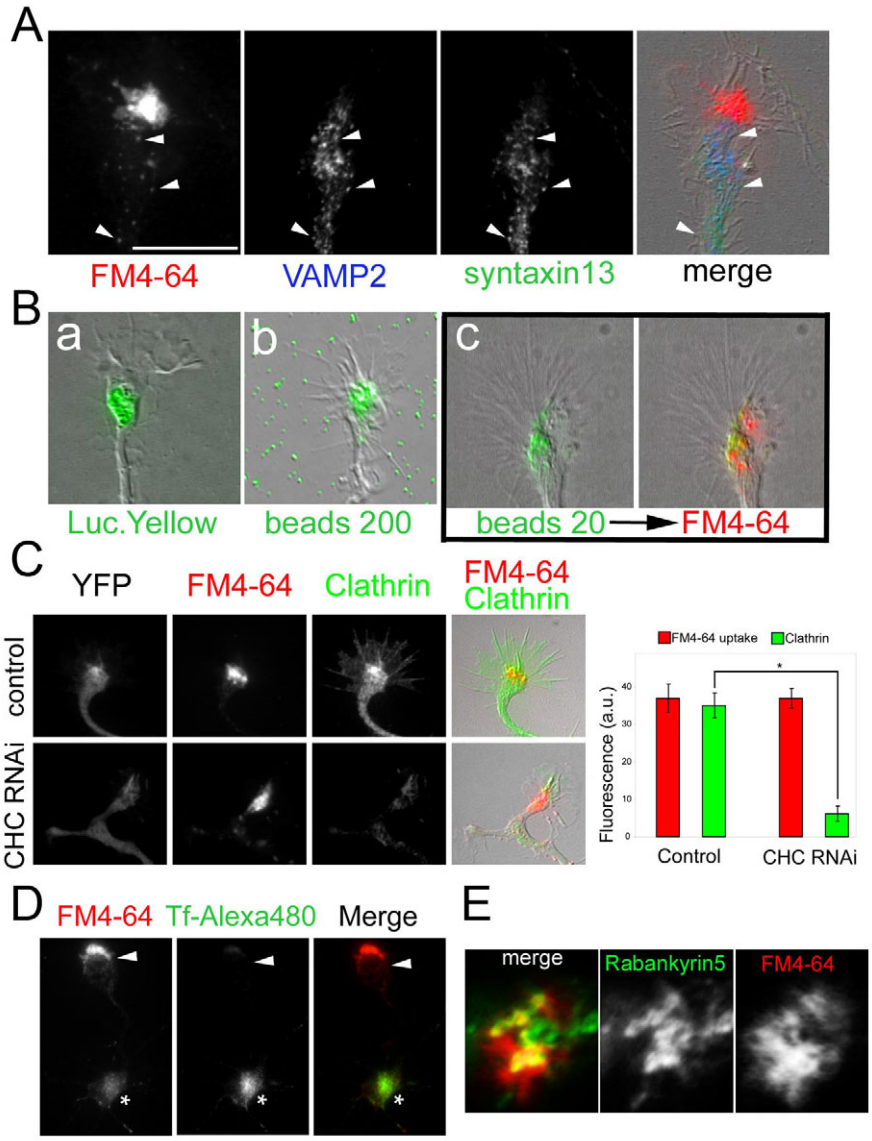

Fig. 4. The high-capacity endocytic process is clathrin-independent and distinct from the SV and endosomal recycling pathways. (A) Basal uptake of FM4-64 (red in the merged image) in a growth cone incubated with the dye for 1 minute, fixed and retrospectively labeled for VAMP2 (blue in the merged image) and syntaxin 13 (green in the merged image). The overlay between the fluorescence and DIC images is shown in the merged image. The bulk of FM4-64 fluorescence colocalizes with neither VAMP2 nor syntaxin 13, although occasional punctae of overlap are observed in more proximal regions (arrowheads). (B) Constitutive endocytosis in growth cones probed by exposure to various tracers (green) for 1 minute in KRH: (a) Lucifer yellow (4 mg/ml), (b) 200-nm beads, (c) 20-nm beads. FM4-64 applied during a subsequent incubation is internalized in bead-containing compartments (right panel in c; red). The overlay between fluorescence and DIC images is shown. (C) Depletion of the clathrin heavy chain (CHC) in mouse hippocampal neurons by RNAi. (Left) Representative images of neurons that were co-transfected with YFP and either control Stealth (upper panels) or CHC Stealth (bottom panels). After basal FM4-64 uptake (red), 3-DIV mouse neurons were fixed and retrospectively immunostained to assess clathrin downregulation (green). (Right) Quantification of the effect of CHC RNAi on bulk plasma-membrane endocytosis. A fivefold reduction of CHC immunoreactivity (green bars; mean ± s.e.m.; n=20 growth cones per treatment) in individual growth cones is observed following RNAi. FM4-64 bulk endocytosis (red bars) is unchanged (*P<0.001, Student's t-test, treated vs control). (D) A neuron exposed to Alexa-Fluor-488-conjugated transferrin (green in the merged image) for 1 hour and subsequently to FM4-64 (red in the merged image) for 1 minute in KRH is shown. Transferrin, which is primarily internalized in the cell body (asterisk), does not overlap with FM4-64, which is endocytosed in the growth cone (arrowhead). (E) Growth cones that were loaded with FM4-64 (KRH, 1 minute; red) and retrospectively stained with anti-Rabankyryn-5 (green in the merged image). Scale bar: 10 µm (A,B); 15 µm (C); 29.5 µm (D); 3.8 µm (E).

internalization in the growth cone. Neurons coexpressing soluble YFP and FLAG-tagged either constitutively active or dominant-negative versions of Rac1 (Rac1-N12 and Rac1-V17, respectively) were exposed to FM4-64 in basal medium. The expression of Rac1 mutants in YFP-positive cells was confirmed by retrospective staining with anti-FLAG antibody. Remarkably, expression of dominant-negative Rac1 dramatically impaired bulk FM4-64 uptake in growth cones. By contrast, the constitutively active Rac1 form did not affect FM4-64 internalization compared with control growth cones expressing only soluble YFP (Fig. 7 and supplementary material Fig. S3). Of note, loading of dye into smaller endocytic organelles was not prevented by Rac1-N17 expression. Rac1-N17 expression led to a reduction in growth-cone size, which could result from a combined action of this protein on the actin cytoskeleton and membrane trafficking (see also Kuhn et al., 1998; Ruchhoeft et al., 1999; Woo and Gomez, 2006).

Pincher regulates bulk plasma-membrane endocytosis

Pincher (also known as Ehd4) is the first regulator of a recently described process of macroendocytosis that underlies ligand-induced internalization and signaling of neurotrophin receptors (Shao et al., 2002; Valdez et al., 2005; Valdez et al., 2007). The involvement of Pincher in constitutive bulk plasma-membrane retrieval in the growth cone was studied by infecting neurons with adenoviruses independently driving expression of GFP and HA-tagged either wild-type or dominant-negative Pincher (Valdez et al., 2005). In a first set of experiments aimed at determining the localization of Pincher in the growth cone, we expressed the exogenous proteins at low levels by reducing both virus concentration and infection times. Infected neurons were exposed for 1 minute to FM4-64 in resting medium and stained with anti-HA antibody to detect either HA-Pincher or HA–Pincher-G68E (Fig. 8A). Pincher showed a partial colocalization with the compartments of FM4-64 uptake. Similar results were obtained when constitutive endocytosis was assayed in HA-Pincher-expressing growth cones by internalization of fluorescent beads (Fig. 8B). By contrast, Pincher G68E displayed a diffuse distribution throughout the growth cone, probably resulting from its irreversible binding to the plasma membrane (Shao et al., 2002) (Fig. 8A). Next, we increased the expression levels of Pincher or Pincher G68E. In growth cones

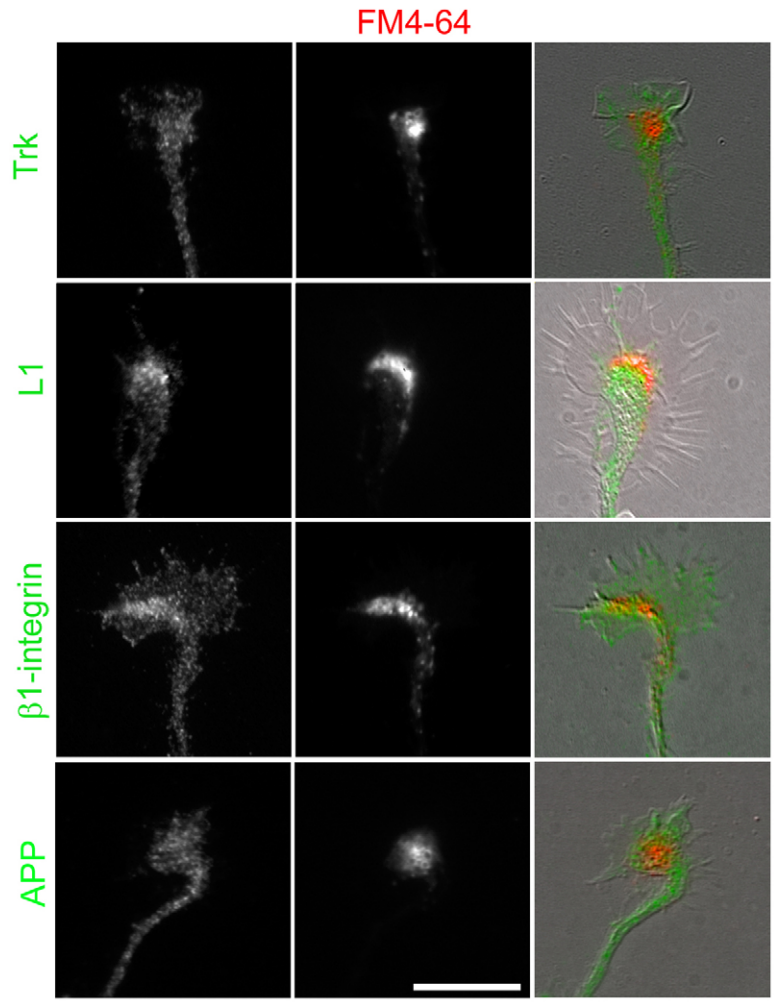

Fig. 5. Exclusion of membrane proteins from bulk endocytosis. Growth cones (2 DIV) incubated in KRH in the presence of FM4-64 (red) for 1 minute, fixed and retrospectively stained with antibodies against integral membrane proteins that are known to undergo recycling in axons (Trk, L1, β1 integrin, APP; green). The overlay between the corresponding fluorescence and DIC images is shown in the right panels. Scale bar: 10 μm.

overexpressing either wild-type or the Pincher-G68E mutant, constitutive FM4-64 uptake was prevented, as compared with either uninfected neurons used as an internal control (Fig. 8C) or neurons infected with adenoviruses expressing only GFP (Fig. 8D,E). The suppression of bulk endocytosis was paralleled by the impairment of axon growth upon overexpression of either wild-type or mutant Pincher, although the latter had a stronger inhibitory effect (Fig. 8F).

As observed with Rac1-N17, smaller endocytic organelles were still loaded with FM4-64 upon overexpression of wild-type or Pincher G68E (Fig. 8D), pointing to the coexistence of at least two mechanistically distinct pathways of constitutive endocytosis in the growth cones.

Developmental control of plasma-membrane endocytosis in the axonal growth cone

To investigate the development-related changes in the membrane-recycling properties at growth cones, we took advantage of the stereotyped and well-characterized sequence of events following the differentiation of hippocampal neurons in culture (Dotti et al., 1988). The effects on growth-cone endocytosis of a depolarizing solution (55 mM KCl) were first investigated at early stages of neuronal differentiation (3 DIV). Growth cones were loaded for 1 minute with FM4-64 in basal medium and subsequently exposed for an additional minute to a high-K^+-containing solution devoid of FM4-64 prior to fixation and staining for VAMP2 (Fig. 9A). K^+ application neither elicited unloading of the dye nor promoted membrane transfer from the compartments of bulk endocytosis to the SV recycling pathway, as indicated by the lack of FM4-64 in the VAMP2-positive SVs. In a second set of experiments, neurons infected with lentiviruses expressing ECFP-tagged VAMP2 (ECFP-VAMP2) were stimulated with high K^+ for 1 minute in the presence of FM4-64. The intensity and pattern of FM4-64 fluorescence after depolarization was remarkably similar to the pattern observed at this stage after constitutive uptake of the dye, being associated with large structures at the distal area of the C domain (Fig. 3C and Fig. 9B, compare with Fig. 1). Importantly, also in this case, no ECFP-VAMP2-positive SVs were labeled by the dye. These results indicate that, at early developmental stages, both bulk plasma-membrane endocytosis and SV recycling are insensitive to depolarizing stimuli.

Growth cones of ECFP-VAMP2-expressing neurons at 4-5 DIV (stage 4, characterized by prominent dendrite outgrowth) (Dotti et al., 1988) were incubated in KRH containing FM4-64 for 1 minute. After a 15-minute interval in basal medium (to unload the internalized dye) followed by photobleaching of the residual fluorescence, the neurons were exposed for 1 minute to a high-K^+-containing solution supplemented with FM4-64. Under resting conditions, uptake of FM4-64 occurred via bulk plasma-membrane internalization separate from SV recycling. The same growth cones,

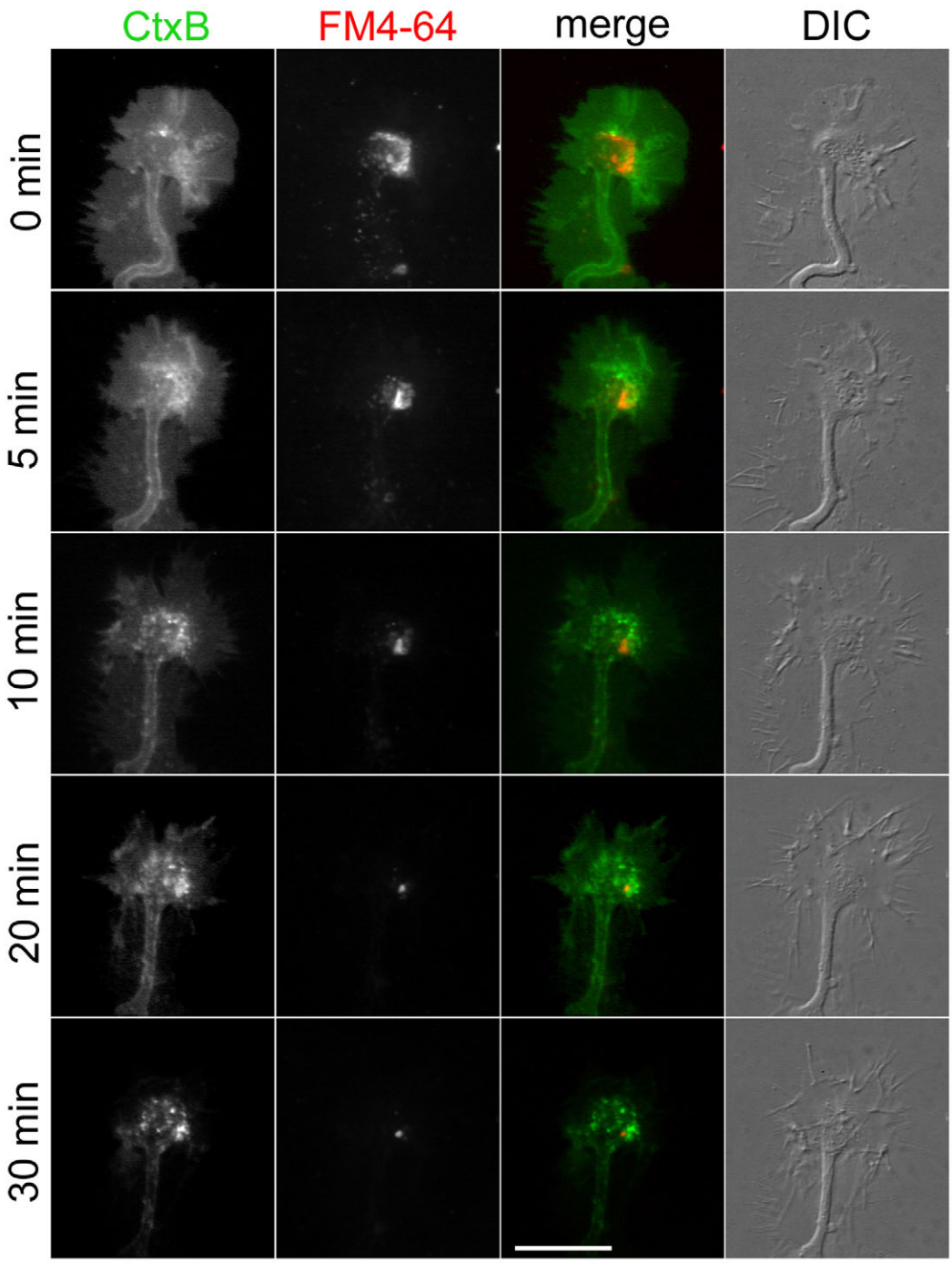

Fig. 6. The pathway of bulk membrane retrieval is distinct from the pathway of cholera-toxin internalization. A growth cone (2 DIV) that was exposed simultaneously to FM4-64 (red in the merged images) and Alexa-Fluor-488-conjugated cholera toxin subunit B (CtxB; green in the merged images) for 1 minute in KRH, washed and imaged during the following 30 minutes at 37°C. Immediately after loading (t=0), FM4-64 is internalized in large compartments, whereas CtxB is still associated with the plasma membrane and is subsequently endocytosed in punctae that do not overlap with FM4-64 labeling. Scale bar: 10 μm.

after application of the depolarizing stimulus, displayed a punctate pattern that was selectively associated with endocytosis of VAMP2-positive SVs (Fig. 10A). Remarkably, bulk endocytosis ceased in growth cones during depolarizing stimuli, which induced SV recycling.

Neurons at 7 DIV display a complex dendritic arbor and a long axon with various branches (stage 5; full maturation) (Dotti et al., 1988). Typically, at this stage, the growth cone that is associated with the main axonal process has already encountered several potential targets, and synaptic contacts have started to be established. Moreover, at this developmental stage the distinctive morphological compartmentalization and dynamics of growth cones are less obvious (our unpublished observations). Upon a 1-minute exposure of 7-DIV neurons to KRH containing FM4-64, the axonal growth cone was largely devoid of FM4-64 labeling, whereas the dye was internalized throughout the soma and neuronal arborization in punctate endocytic structures that did not overlap with synaptic terminals (Fig. 10B and data not shown). When neurons at 7 DIV were exposed to FM4-64 during a 1-minute depolarization with high K^+, the dye was loaded in ECFP-VAMP2-positive SVs at both growth cones and synapses (Fig. 10C and data not shown).

The extent of the developmental suppression of bulk membrane retrieval was measured in neurons at 3, 5 and 7 DIV that were

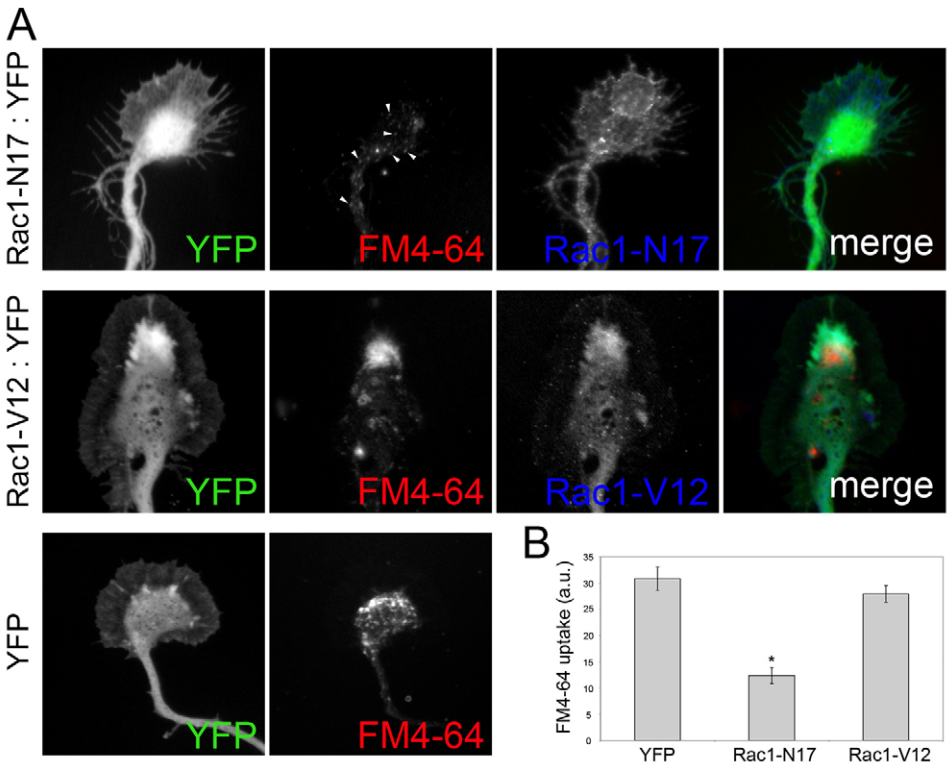

Fig. 7. Rac1 activity is required for bulk plasma-membrane endocytosis in the growth cones. (A) Growth cones of 3-DIV neurons coexpressing YFP (green in the merged images) and either the dominant-negative mutant Rac1-N17 (top panels) or the constitutively active mutant Rac1-V12 (middle panels), or expressing only YFP (bottom panels), incubated in KRH containing FM4-64 (red in the merged images) for 1 minute and fixed. The Rac1 mutants are detected with an anti-FLAG antibody (blue in the merged images). Expression of Rac1-N17 inhibits bulk FM4-64 internalization whereas endocytosis via smaller vesicles is unaffected (arrowheads). (B) Quantification of FM4-64 uptake in Rac1-N17- or Rac1-V12-expressing growth cones treated as shown in A (mean ± s.e.m.; n=27 growth cones per condition; *P<0.001, Dunnett's test for neurons expressing either Rac1-N17 or Rac1-V12 vs control, i.e. growth cones expressing YFP only). The total growth-cone area was reduced by Rac1-N17 expression (mean ± s.e.m.: control, 44±2.5 μm^2; Rac1-N17, 35±2.6 μm^2; P<0.05, Dunnett's test vs control), but not by Rac1-V12 expression (mean ± s.e.m.: 42±2.7 μm^2). Scale bar: 10 μm.

exposed to FM4-64 in basal medium (1 minute) and subsequently depolarized to exclude any contribution of activity-dependent endocytic pathways. These studies showed that bulk constitutive plasma-membrane retrieval that is associated with growth cones is progressively downregulated during neuronal differentiation (Fig. 10D and Fig. 11). In addition, SVs, which appear to be reluctant to undergo both spontaneous and evoked exo-endocytosis at early developmental stages, become competent for depolarization-induced recycling at later stages.

Discussion

In this study we identify a novel process of bulk plasma-membrane retrieval as the main pathway of constitutive endocytosis in growth cones at early stages of neuronal differentiation. Neither the classical endosomal system nor SVs participate in high-volume endocytosis of the growth-cone plasmalemma, which involves large compartments associated with sites of intense actin-based membrane ruffling. Our results provide an explanation for the previous identification of the growth cone as the major site of axonal endocytosis (Sinclair et al., 1988; Parton et al., 1992; Zakharenko and Popov, 2000; Pfenninger and Maylié-Pfenninger, 1981; Cheng and Reese, 1987). In addition, we show that basal endocytosis is preferentially associated with highly motile growth cones during early periods of development, which are characterized by intense axonal growth, and is downregulated at the onset of synaptogenesis, concomitantly with the appearance of depolarization-induced SV recycling.

Because growth cones undergo constant morphological remodeling during guidance and target recognition (Mason and Erskine, 2000), the axonal sensor apparatus needs continuous renewal by insertion and removal of proteins to adjust its sensitivity to environmental cues (Vogt et al., 1996; van Horck et al., 2004). The new membrane-retrieval pathway described in this study might account for the efficient remodeling of the growth-cone membrane during the early stages of neuronal development.

FM4-64 uptake is not affected by prolonged incubation of neurons in the presence of BFA, which arrests trafficking of Golgi-derived vesicles and axon elongation but not growth-cone motility (Craig et al., 1995; Jareb and Banker, 1997). Hence, bulk constitutive endocytosis appears to reflect a local recycling activity of the growth cone, which can occur independently of the supply of new membrane from the cell body, contributing to homeostasis of the axonal plasma membrane. The bulk endocytic process might provide the growth cone with a reservoir of ready-to-use membrane to be added to the cell surface to rapidly reconfigure and update the plasma-membrane make-up during pathfinding and establishment of contacts with targets. In addition, it is possible that such bulk endocytosis enables the growth cone to sample extracellular proteins in a non-specific fashion to be retrogradely transported to the cell body (von Bartheld, 2004).

Constitutive membrane retrieval in the growth cone appears to be mechanistically related to macropinocytosis, a form of high-volume, clathrin-independent endocytosis described in various cell types and particularly well-characterized in macrophages and dendritic cells (Swanson and Watts, 1995; Johannes and Lamaze, 2002; Kirkham and Parton, 2005). Macropinosomes are generated when membrane protrusions that form during actin-based ruffling fuse back with the plasma membrane, trapping fluid-phase material. Striking similarities between bulk membrane retrieval in the growth cone and macropinocytosis include the association with membrane ruffling, the involvement of pleiomorphic endocytic structures of large size, the dependence on actin dynamics, the requirement of PI3-kinase activity, the sensitivity to cholesterol depletion and the involvement of the small GTPase Rac1 (Swanson and Watts, 1995; Johannes and Lamaze, 2002;

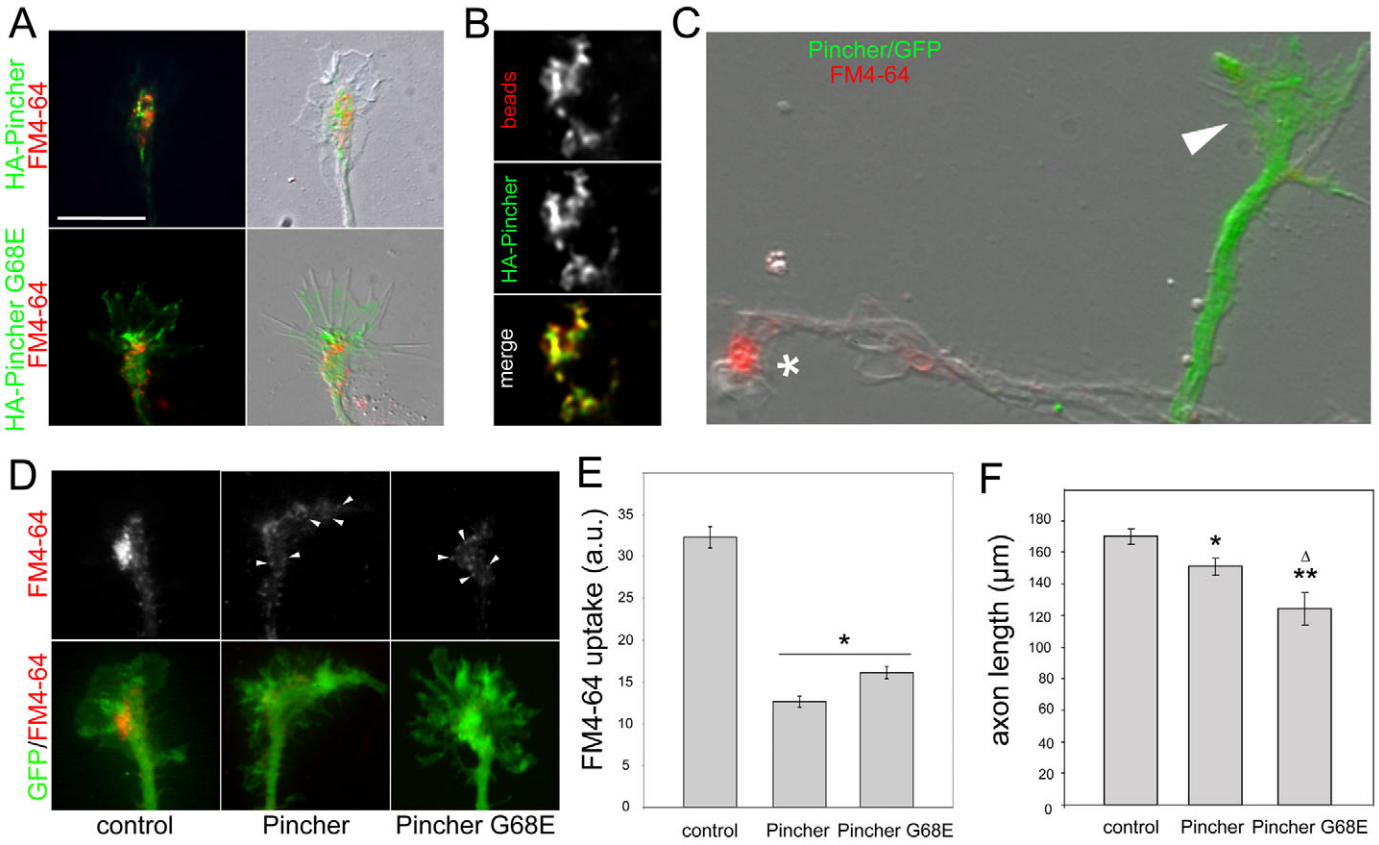

Fig. 8. The marker of neuronal macroendocytosis, Pincher, regulates constitutive plasma-membrane retrieval at the growth cone. Growth cones of neurons at 3 DIV that were infected with adenoviruses driving the simultaneous expression of GFP and either HA-Pincher or HA–Pincher-G68E are shown. (A) Growth cones expressing low levels of HA-Pincher or HA–Pincher-G68E that were stained with anti-HA antibody (green) after basal FM4-64 (red) uptake (1 minute) to reveal the distribution of the exogenous proteins. The overlay between the fluorescence and DIC images is shown in the right panels. (B) Growth cone expressing HA-Pincher at low levels exposed to 20-nm beads (red in the merged image) for 1 minute in KRH, fixed and stained with anti-HA antibody (green in the merged image). The images are maximal projections of deconvoluted *z*-stacks. Pincher overlaps with the compartments of bulk endocytosis. (C,D) Basal FM4-64 uptake (1 minute) in growth cones overexpressing GFP and either HA-Pincher or HA–Pincher-G68E, or infected with adenoviruses expressing only GFP (control). (C) Shows the overlay between the fluorescence and DIC images of a HA-Pincher/GFP-expressing growth cone (arrowhead) and of an uninfected growth cone (asterisk) located in the same field of view. Overexpression of either Pincher or the dominant-negative mutant Pincher G68E inhibits constitutive bulk plasma-membrane uptake, whereas endocytosis via smaller vesicles is unaffected (arrowheads in D). (E) Quantification of FM4-64 uptake in HA-Pincher- or HA–Pincher-G68E-expressing growth cones (mean ± s.e.m.; n=50 growth cones per condition; *P<0.001, Dunnett's test vs control, i.e. growth cones expressing only GFP). Expression of either mutant does not affect the total growth-cone area (P>0.05, Dunnett's test vs control). (F) Quantification of axon length in 2-DIV neurons that were nucleofected with GFP alone (control) or together with either HA-Pincher or HA–Pincher-G68E. The length of the longest neurite, corresponding to the axonal process, was measured for each transfected neuron (mean ± s.e.m.; n=100-150 growth cones per condition from three independent experiments; **P<0.001, Tukey's test Pincher G68E vs control; *P<0.05, Pincher wild-type vs control; $^{\Delta}P$<0.05, Pincher wild-type vs Pincher G68E). Scale bar: 10 µm (A,C,D); 3.3 µm (B).

Kirkham and Parton, 2005; Lindmo and Stenmark, 2006). In the growth cone, the role of PI3-kinase and Rac1 in bulk plasma-membrane retrieval is plausibly linked to the remodeling of the subcortical actin cytoskeleton, controlled by PI3-kinase via PtdIns(3,4,5)P_3 effectors, including the small GTPases Rac1, Cdc42 and Arf6 (Govek et al., 2005; Lindmo and Stenmark, 2006). Yet, the compartments of bulk endocytosis in the growth cone do not overlap with the distribution of GM1, which is enriched in macropinosomes in non-neuronal cells (Watarai et al., 2001), and show only partial colocalization with Rabankyrin-5 (Schnatwinkel et al., 2004). Of note, various integral proteins of the growth-cone plasma membrane are excluded from bulk endocytosis, in analogy with the sorting process that accompanies macropinosome formation (Mercanti et al., 2006). Sorting is conceivably required to preserve the specific composition of both the plasma membrane and intracellular compartments.

Our results extend the role of the chaperone Pincher to the control of constitutive membrane retrieval at the growth cone. Pincher mediates ligand-stimulated, clathrin-independent endocytosis of neurotrophin receptors through macroendosomes generated at sites of plasma-membrane ruffling (Shao et al., 2002; Valdez et al., 2005; Valdez et al., 2007). Overexpression of either wild-type or dominant-negative Pincher interfered with bulk FM4-64 uptake. It is possible that the effect of high doses of wild-type Pincher reflects the exhaustion of basal endocytic activity following an early phase of accelerated membrane retrieval that might have escaped detection in our assay.

During development, an intrinsic program of maturation appears to contribute to changing the endocytic properties of growth cones (Fig. 11). Remarkably, depolarization of mature (stage 4) growth cones induces selective internalization of the dye in SVs but not in the large compartments labeled at rest. This situation is reminiscent

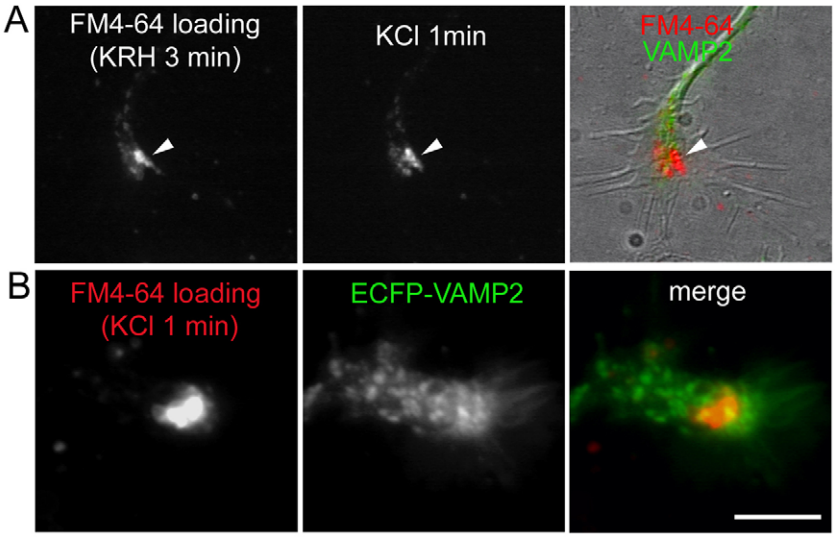

Fig. 9. Plasma-membrane endocytosis in growth cones at early developmental stages is insensitive to depolarizing stimuli. (A) Uptake of FM4-64 (red in the merged image, arrowhead) in a growth cone of a 2-DIV neuron incubated with the dye for 3 minutes in KRH (left), followed by incubation with high K^+ for 1 minute (middle). After depolarization, the growth cone was fixed and retrospectively stained for VAMP2 (green). In the right panel the overlay between the fluorescence and DIC images is shown. (B) Growth cone of a 2-DIV neuron expressing ECFP-VAMP2 (green in the merged image) incubated with high K^+ for 1 minute in the presence of FM4-64 (red in the merged image). VAMP2-positive SVs do not internalize FM4-64 upon depolarization. Scale bar: 10 µm (A); 5.5 µm (B).

of the spatial and temporal dissociation between bulk compensatory endocytosis and SV recycling previously reported at the ribbon synapse of retinal bipolar cells (Holt et al., 2003). Whereas the switch in the sensitivity of growth cones to depolarization is likely to reflect developmental changes in the Ca^{2+}-sensing apparatus (Pravettoni et al., 2000; Menegon et al., 2002), dissociation of basal bulk endocytosis from depolarization-induced SV endocytosis could represent a way to uncouple major rearrangements of the plasma membrane from ongoing SV recycling, thus preserving the molecular identity of the SV pool. Indeed, both bulk membrane endocytosis and SV recycling take place preferentially in the T zone of growth cones (Bonanomi et al., 2005).

The mechanism(s) targeted to occlude bulk membrane retrieval in mature neurons is unknown. One attractive possibility is that, during synaptogenesis, spontaneous network activity generates 'maturation' signals that locally repress the PI3-kinase–Rac1–F-actin machinery in the growth cone. This control might be exerted at different levels, for instance involving guanine-nucleotide exchange factors (GEFs) and/or GTPase-activating proteins (GAPs), which tune Rac1 activity. A similar working model might explain the effect of depolarization on isolated stage-4 growth cones. At this stage, growth cones, which appear to have already acquired the molecular apparatus to sense developmental signals and repress bulk uptake, still lack actual maturation inputs from the forming network. Interestingly, constitutive macropinocytosis, which is downregulated in mature dendritic cells that have initiated the processing of an acquired antigen, can be restored upon expression of active forms of Rac and Cdc42 (Garrett et al., 2000). In an alternative model, during neuronal differentiation, bulk membrane retrieval might be replaced by selective retrieval directed by factors such as the neurotrophins, via a similar Rac- and Pincher-dependent pathway (Valdez et al., 2007).

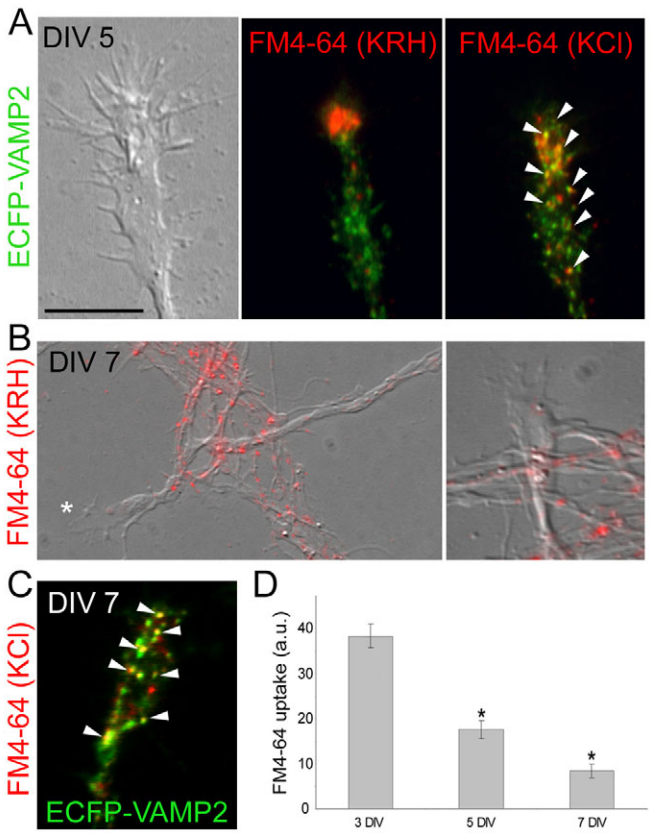

Fig. 10. Developmental control of endocytic activities in the growth cone. (A) Growth cone (DIC, left) of a neuron at 5 DIV expressing ECFP-VAMP2 (green) that was subjected to two 15-minute-spaced applications of FM4-64 (red) for 1 minute in either KRH (first application, middle) or high K^+ (second application, right). The depolarizing step induces FM4-64 loading in VAMP2-positive SVs (arrowheads) with a pattern that is markedly different from that of constitutive endocytic compartments. (B) Neurons at 7 DIV that were incubated with FM4-64 for 1 minute in KRH. At this stage, constitutive FM4-64 uptake is not associated with growth cones (asterisk), whereas it is present in punctate endocytic compartments along the neurite network. (C) Growth cone of a 7-DIV neuron expressing ECFP-VAMP2 (green) incubated with high K^+ for 1 minute in the presence of FM4-64 (red). Arrowheads point to VAMP2-positive SVs that internalized the dye upon depolarization. (D) Quantification of basal FM4-64 uptake in growth cones of neurons at 3, 5 and 7 DIV incubated with FM4-64/KRH for 1 minute, rapidly washed and then exposed to high K^+ for 1 minute. Bulk endocytosis is suppressed at later developmental stages (mean ± s.e.m.; n=30-40 growth cones per treatment). At all time points, FM4-64 uptake was significantly different (P<0.001, Tukey's test). Scale bar: 7 µm (A,C); 12.5 µm (B, left); 7.5 µm (B, right).

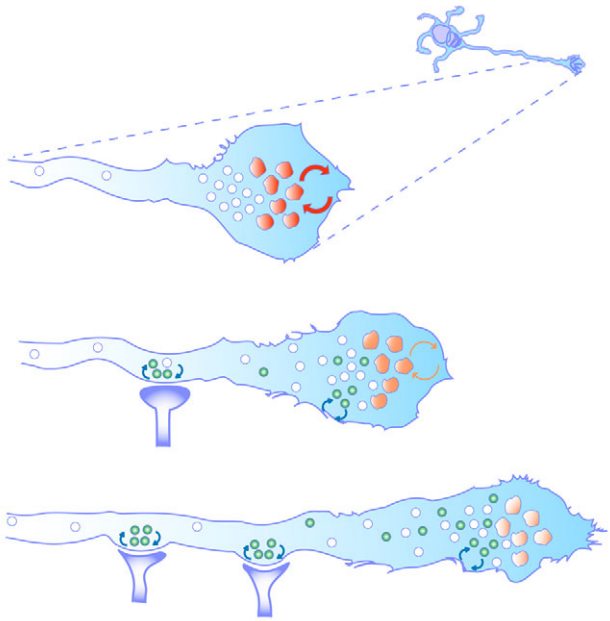

Fig. 11. Developmental changes in the endocytic properties of the growth cone. Top: at early stages of differentiation (3 DIV), constitutive high-capacity plasma-membrane recycling occurs via a bulk endocytic pathway mediated by large compartments (red) in the T domain of the growth cone. SV precursors (white circles), which, at these stages, are not prone to either constitutive or evoked recycling, do not participate in the bulk retrieval process. Middle: as neuronal differentiation proceeds (4-5 DIV), the intensity of the bulk recycling process decreases (orange) concomitantly with the emergence of activity-dependent SV recycling (green circles) in both the growth cone and nascent synaptic structures. Bottom: bulk plasma-membrane retrieval ceases at later stages of neuronal differentiation (7 DIV), when frequent interactions of the growth cone with targets result in the establishment of synaptic contacts associated with robust activity-dependent SV recycling. Exo-endocytosis of SVs is maintained also in the growth cone. The dissociation of bulk endocytosis from the SV recycling pathway at the onset of synaptogenesis might preserve the molecular identity of the forming pool of SVs and the stability of nascent synaptic structures.

Materials and Methods

Materials

The following primary antibodies were used: mouse anti-synaptobrevin-2, rabbit anti-APP and rabbit anti-syntaxin-13 (Synaptic Systems, Göttingen, Germany); mouse anti-Tau-1 (MAB3420) (Millipore Corporation, Billerica, MA); mouse anti-CHC (clone X22) (ABR-Affinity BioReagents, Golden, CO); mouse anti-hemagglutinin (HA) (Roche Diagnostics, Indianapolis, IN); rabbit anti-panTrk (C-14) (Santa Cruz Biotechnology, Santa Cruz, CA); mouse anti-FLAG M5 (Sigma-Aldrich, St Louis, MO); rabbit anti-L1 (a gift of F. Rathjen, Max-Delbrueck-Centrum fuer Molekulare Medizin, Berlin, Germany), rabbit anti-Rabankyrin-5 (a gift of M. Zerial, MPI Molecular Cell Biology and Genetics, Dresden, Germany); rabbit anti-β1-integrin (a gift from K. Rubin, Uppsala University, Uppsala, Sweden). TRITC- and FITC-conjugated secondary antibodies were from Jackson ImmunoResearch (West Grove, PA). FITC-conjugated phalloidin, filipin III, Lucifer yellow CH, brefeldin A (BFA), LY294002 and MβCD were from Sigma-Aldrich (St Louis, MO). FM4-64, yellow-green (505/515) carboxylate-modified FluoSpheres beads, transferrin–Alexa-Fluor-488, CtxB–Alexa-Fluor-488 were from Invitrogen-Molecular Probes (Carlsbad, CA). Cytochalasin D was from Calbiochem (La Jolla, CA). All chemicals were diluted in KRH (in mM: 150 NaCl, 5 KCl, 1.2 $MgSO_4$, 1.2 KH_2PO_4, 2 $CaCl_2$, 10 glucose and 10 HEPES, pH 7.4) at the concentrations indicated in the figures. For depletion of extracellular Ca^{2+}, KRH was supplemented with 2 mM EGTA and $CaCl_2$ was substituted with 2 mM $MgCl_2$.

Plasmids and viral vectors

The pFLAG-N17-Rac1A plasmid coding for the dominant-negative form of the avian Rac1A GTPase, and the pFLAG-V12-Rac1A plasmid coding for the constitutively active form of the Rac GTPases were a gift of Ivan de Curtis (DIBIT-San Raffaele Scientific Institute, Milan, Italy) (Albertinazzi et al., 1998). The pEYFP-N3 vector was from BD Biosciences Clontech (Palo Alto, CA). Lentiviruses expressing ECFP-VAMP2 have been previously described (Bonanomi et al., 2005). Defective recombinant adenoviruses driving the simultaneous expression of GFP and either HA-Pincher or HA–Pincher-G68E were made using the Ad-Easy system (Valdez et al, 2005). Adenoviruses expressing GFP have been produced at the AAV Vector Unit (AVU) of the International Centre for Genetic Engineering and Biotechnology (ICGEB), Trieste, Italy, as previously described (Zentilin et al., 2001).

RNA interference

The CHC Stealth RNAi (Invitrogen, Carlsbad, CA) efficiently knocks down clathrin in mouse cells (Lampugnani et al., 2006). Stealth were designed with the BLOCK-iT RNAi Designer (Invitrogen, Carlsbad, CA), starting from *Mus musculus* clathrin, heavy polypeptide NM_001003908. The starting nucleotide is 1284 bases downstream of the start codon (5′-3′ sequence GAAGAACUCUUUGCCCGGAAAUUUA, antisense UAAAUUUCCGGGCAAAGAGUUCUUC). As a control, a Stealth siRNA-negative control duplex oligonucleotide with a C/G content equivalent to the positive oligonucleotide was used (5′-3′ sequence GAAUCAUUCCGUGC-CAAGUAGAUUA, antisense UAAUCUACUUGGCACGGAAUGAUUC). After dissection and trypsinization, mouse neurons were nucleofected as described below and cultured for 48 hours before the experiments. Efficient silencing was verified by retrospective immunofluorescence.

Cell culture and transduction of neurons

Primary neuronal cultures were prepared from the hippocampi of either Sprague-Dawley E18 rat embryos or E17 C57BL/6J mouse embryos (Charles River Italica, Calco, Italy) as previously described (Banker and Cowan, 1977). For infection, neurons were placed the day after plating in a clean dish containing glia-conditioned medium [MEM supplemented with 1% N2 supplement (Invitrogen), 2 mM glutamine (Biowhittaker, Walkersville, MD), 0.1% ovalbumin, 1 mM sodium pyruvate (Sigma-Aldrich) and 4 mM glucose] and incubated for 10-15 hours at 37°C in a 5% CO_2 humidified atmosphere in the presence of viral supernatant. After transduction, neurons were returned to the original dishes and maintained in culture in glia-conditioned medium. In some experiments, rat neurons (~1.5×10^6 cells) were nucleofected in suspension with 3 μg of DNA immediately after harvesting, using the Basic Nucleofector Kit for primary neurons (Amaxa Biosystems, Cologne, Germany) (O-03 program). For RNAi experiments, mouse neurons (~3×10^6 cells) were nucleofected with 3 μg of oligonucleotides together with 0.5 μg pEYFP-N3 plasmid using the O-05 program. After electroporation, neurons were diluted and plated at the standard low density.

Cell-labeling protocols

For FM4-64-uptake experiments, neurons were incubated with FM4-64 (10 μM) diluted in either KRH (basal medium) or KRH containing 55 mM KCl (depolarizing solution) for 1 minute at room temperature (RT), rinsed three times by complete medium substitution with KRH over a course of 2 minutes and live imaged. When indicated, FM4-64 uptake was carried out at 37°C. Because fixation does not result in noticeable loss of FM4-64 fluorescence (Diefenbach et al., 1999), in several experiments neurons were fixed after loading with FM4-64 in order to obtain large numbers of growth cones for analysis. Fixation was performed for 15 minutes at RT with 4% paraformaldehyde, 4% sucrose in 120 mM sodium phosphate buffer (pH 7.4) supplemented with 2 mM EGTA. In some cases, fixed neurons were processed for immunofluorescence as previously described (Menegon et al., 2002). Because FM4-64 is lost upon cell permeabilization, a circle was inscribed on the bottom coverslip using a diamond-tip scribing objective (Zeiss, Oberkochen, Germany) and was used as a reference to relocate previously imaged growth cones. For loading of fluorescent polystyrene beads, neurons were incubated with 1 μl of an aqueous suspension containing 2% solids diluted in 1 ml KRH.

Videomicroscopy and image analysis

Specimens were viewed with an Axiovert 135 inverted microscope (Zeiss, Oberkochen, Germany) equipped with epifluorescence optics. Images were recorded with a C4742-98 ORCA II cooled charge-coupled device camera (Hamamatsu Photonics, Hamamatsu City, Japan) and processed using Image Pro Plus 4.5 (Media Cybernetics, Silver Spring, MD) and Adobe Photoshop 6.0 (Adobe System, San Jose, CA). For image deconvolution, *z*-stacks of optical sections taken withOlympus IX70 with DeltaVision RT Deconvolution System (Olympus, Hamburg, Germany) were analyzed by the WoRx Deconvolve software (Applied Precision, Issaquah, WA). In order to quantify the FM4-64 signal in individual growth cones, images were acquired at constant parameters of illumination and gain, and the specific fluorescence intensity, calculated by subtracting a fixed fluorescence background level from the total pixel intensity, was measured within the whole growth-cone area determined by either DIC or GFP/YFP fluorescence images. For the analysis of growth-cone motility, neurons were imaged in a temperature-controlled heated chamber with an inverted Olympus IX81 microscope (Hamburg, Germany). Images were taken every 30 seconds for 6 minutes. Quantification of cone dynamics was performed using a custom-made macro for NIH ImageJ that calculates differences in growth-cone area in consecutive time frames. The motility index is then calculated as the summation of differences in areas

divided by the frequency of sampling. One-way ANOVA followed by either Dunnett's or Tukey's multiple comparison tests were used and P values <0.05 were considered significant.

We wish to thank Ivan de Curtis and Jacopo Meldolesi (S. Raffaele Scientific Institute/Vita-Salute University, Milano, Italy) for critical reading of the manuscript. We also thank Lorena Zentilin and the Telethon AVU Core Facility for the generous gift of the GFP-adeno-associated virus and Ivan de Curtis for the Rac1 constructs. This work was supported by grants from the Italian Ministry of University (Cofin 2005 and 2006 to F.V. and F.B., respectively), from the CARIPLO Foundation and from the Mariani Foundation for Infantile Neurology (to F.V. and F.B). The financial support of Telethon-Italy (grant number GGP05134 to F.B and F.V.) and Compagnia di San Paolo (to F.B.) is gratefully acknowledged.

References

Ahmari, S. E., Buchanan, J. and Smith, S. J. (2000). Assembly of presynaptic active zones from cytoplasmic transport packets. *Nat. Neurosci.* **3**, 445-451.

Albertinazzi, C., Gilardelli, D., Paris, S., Longhi, R. and de Curtis, I. (1998). Overexpression of a neural-specific rho family GTPase, cRac1B, selectively induces enhanced neuritogenesis and neurite branching in primary neurons. *J. Cell Biol.* **142**, 815-825.

Albertinazzi, C., Za, L., Paris, S. and de Curtis, I. (2003). ADP-ribosylation factor 6 and a functional PIX/p95-APP1 complex are required for Rac1B-mediated neurite outgrowth. *Mol. Biol. Cell* **14**, 1295-1307.

Ashery, U., Penner, R. and Spira, M. E. (1996). Acceleration of membrane recycling by axotomy of cultured aplysia neurons. *Neuron* **16**, 641-651.

Banker, G. A. and Cowan, W. M. (1977). Rat hippocampal neurons in dispersed cell culture. *Brain Res.* **126**, 397-442.

Betz, W. J. and Bewick, G. S. (1992). Optical analysis of synaptic vesicle recycling at the frog neuromuscular junction. *Science* **255**, 200-203.

Betz, W. J., Mao, F. and Smith, C. B. (1996). Imaging exocytosis and endocytosis. *Curr. Opin. Neurobiol.* **6**, 365-371.

Bonanomi, D., Menegon, A., Miccio, A., Ferrari, G., Corradi, A., Kao, H. T., Benfenati, F. and Valtorta, F. (2005). Phosphorylation of synapsin I by cAMP-dependent protein kinase controls synaptic vesicle dynamics in developing neurons. *J. Neurosci.* **25**, 7299-7308.

Bonanomi, D., Benfenati, F. and Valtorta, F. (2006). Protein sorting in the synaptic vesicle life cycle. *Prog. Neurobiol.* **80**, 177-217.

Bray, D. (1970). Surface movements during the growth of single explanted neurons. *Proc. Natl. Acad. Sci. USA* **65**, 905-910.

Chen, Z. Y., Ieraci, A., Tanowitz, M. and Lee, F. S. (2005). A novel endocytic recycling signal distinguishes biological responses of trk neurotrophin receptors. *Mol. Biol. Cell* **16**, 5761-5772.

Cheng, T. P. and Reese, T. S. (1985). Polarized compartmentalization of organelles in growth cones from developing optic tectum. *J. Cell Biol.* **101**, 1473-1480.

Cheng, T. P. and Reese, T. S. (1987). Recycling of plasmalemma in chick tectal growth cones. *J. Neurosci.* **7**, 1752-1759.

Chow, I. and Poo, M. M. (1985). Release of acetylcholine from embryonic neurons upon contact with muscle cell. *J. Neurosci.* **5**, 1076-1082.

Cohen, J. E. and Fields, R. D. (2006). CaMKII inactivation by extracellular ca(2+) depletion in dorsal root ganglion neurons. *Cell Calcium* **39**, 445-454.

Condic, M. L. and Letourneau, P. C. (1997). Ligand-induced changes in integrin expression regulate neuronal adhesion and neurite outgrowth. *Nature* **389**, 852-856.

Craig, A. M., Wyborski, R. J. and Banker, G. (1995). Preferential addition of newly synthesized membrane protein at axonal growth cones. *Nature* **375**, 592-594.

Dailey, M. E. and Bridgman, P. C. (1989). Dynamics of the endoplasmic reticulum and other membranous organelles in growth cones of cultured neurons. *J. Neurosci.* **9**, 1897-1909.

Dent, E. W. and Gertler, F. B. (2003). Cytoskeletal dynamics and transport in growth cone motility and axon guidance. *Neuron* **40**, 209-227.

Diefenbach, T. J., Guthrie, P. B., Stier, H., Billups, B. and Kater, S. B. (1999). Membrane recycling in the neuronal growth cone revealed by FM1-43 labeling. *J. Neurosci.* **19**, 9436-9444.

Dotti, C. G., Sullivan, C. A. and Banker, G. A. (1988). The establishment of polarity by hippocampal neurons in culture. *J. Neurosci.* **8**, 1454-1468.

Falcone, S., Cocucci, E., Podini, P., Kirchhausen, T., Clementi, E. and Meldolesi, J. (2006). Macropinocytosis: regulated coordination of endocytic and exocytic membrane traffic events. *J. Cell. Sci.* **119**, 4758-4769.

Fletcher, T. L., Cameron, P., De Camilli, P. and Banker, G. (1991). The distribution of synapsin I and synaptophysin in hippocampal neurons developing in culture. *J. Neurosci.* **11**, 1617-1626.

Forscher, P. and Smith, S. J. (1988). Actions of cytochalasins on the organization of actin filaments and microtubules in a neuronal growth cone. *J. Cell Biol.* **107**, 1505-1516.

Forscher, P., Lin, C. H. and Thompson, C. (1992). Novel form of growth cone motility involving site-directed actin filament assembly. *Nature* **357**, 515-518.

Fournier, A. E., Nakamura, F., Kawamoto, S., Goshima, Y., Kalb, R. G. and Strittmatter, S. M. (2000). Semaphorin3A enhances endocytosis at sites of receptor-F-actin colocalization during growth cone collapse. *J. Cell Biol.* **149**, 411-422.

Garrett, W. S., Chen, L. M., Kroschewski, R., Ebersold, M., Turley, S., Trombetta, S., Galan, J. E. and Mellman, I. (2000). Developmental control of endocytosis in dendritic cells by Cdc42. *Cell* **102**, 325-334.

Govek, E. E., Newey, S. E. and Van Aelst, L. (2005). The role of the rho GTPases in neuronal development. *Genes Dev.* **19**, 1-49.

Granseth, B., Odermatt, B., Royle, S. J. and Lagnado, L. (2006). Clathrin-mediated endocytosis is the dominant mechanism of vesicle retrieval at hippocampal synapses. *Neuron* **51**, 773-786.

Holt, M., Cooke, A., Wu, M. M. and Lagnado, L. (2003). Bulk membrane retrieval in the synaptic terminal of retinal bipolar cells. *J. Neurosci.* **23**, 1329-1339.

Jareb, M. and Banker, G. (1997). Inhibition of axonal growth by brefeldin A in hippocampal neurons in culture. *J. Neurosci.* **17**, 8955-8963.

Johannes, L. and Lamaze, C. (2002). Clathrin-dependent or not: is it still the question? *Traffic* **3**, 443-451.

Jurney, W. M., Gallo, G., Letourneau, P. C. and McLoon, S. C. (2002). Rac1-mediated endocytosis during ephrin-A2- and semaphorin 3A-induced growth cone collapse. *J. Neurosci.* **22**, 6019-6028.

Kamiguchi, H. and Lemmon, V. (2000). Recycling of the cell adhesion molecule L1 in axonal growth cones. *J. Neurosci.* **20**, 3676-3686.

Kim, Y. T. and Wu, C. F. (1987). Reversible blockage of neurite development and growth cone formation in neuronal cultures of a temperature-sensitive mutant of drosophila. *J. Neurosci.* **7**, 3245-3255.

Kirkham, M. and Parton, R. G. (2005). Clathrin-independent endocytosis: new insights into caveolae and non-caveolar lipid raft carriers. *Biochim. Biophys. Acta* **1745**, 273-286.

Kirkham, M., Fujita, A., Chadda, R., Nixon, S. J., Kurzchalia, T. V., Sharma, D. K., Pagano, R. E., Hancock, J. F., Mayor, S. and Parton, R. G. (2005). Ultrastructural identification of uncoated caveolin-independent early endocytic vehicles. *J. Cell Biol.* **168**, 465-476.

Kuhn, T. B., Brown, M. D. and Bamburg, J. R. (1998). Rac1-dependent actin filament organization in growth cones is necessary for beta1-integrin-mediated advance but not for growth on poly-D-lysine. *J. Neurobiol.* **37**, 524-540.

Lampugnani, M. G., Orsenigo, F., Gagliani, M. C., Tacchetti, C. and Dejana, E. (2006). Vascular endothelial cadherin controls VEGFR-2 internalization and signaling from intracellular compartments. *J. Cell Biol.* **174**, 593-604.

Leoni, C., Menegon, A., Benfenati, F., Toniolo, D., Pennuto, M. and Valtorta, F. (1999). Neurite extension occurs in the absence of regulated exocytosis in PC12 subclones. *Mol. Biol. Cell* **10**, 2919-2931.

Lindmo, K. and Stenmark, H. (2006). Regulation of membrane traffic by phosphoinositide 3-kinases. *J. Cell. Sci.* **119**, 605-614.

Lippincott-Schwartz, J., Yuan, L. C., Bonifacino, J. S. and Klausner, R. D. (1989). Rapid redistribution of golgi proteins into the ER in cells treated with brefeldin A: Evidence for membrane cycling from golgi to ER. *Cell* **56**, 801-813.

Lockerbie, R. O., Miller, V. E. and Pfenninger, K. H. (1991). Regulated plasmalemmal expansion in nerve growth cones. *J. Cell Biol.* **112**, 1215-1227.

Mason, C. and Erskine, L. (2000). Growth cone form, behavior, and interactions *in vivo*: retinal axon pathfinding as a model. *J. Neurobiol.* **44**, 260-270.

Matteoli, M., Takei, K., Perin, M. S., Südhof, T. C. and De Camilli, P. (1992). Exo-endocytotic recycling of synaptic vesicles in developing processes of cultured hippocampal neurons. *J. Cell Biol.* **117**, 849-861.

Menegon, A., Verderio, C., Leoni, C., Benfenati, F., Czernik, A. J., Greengard, P., Matteoli, M. and Valtorta, F. (2002). Spatial and temporal regulation of Ca2+/calmodulin-dependent protein kinase II activity in developing neurons. *J. Neurosci.* **22**, 7016-7026.

Mercanti, V., Charette, S. J., Bennett, N., Ryckewaert, J. J., Letourneur, F. and Cosson, P. (2006). Selective membrane exclusion in phagocytic and macropinocytic cups. *J. Cell. Sci.* **119**, 4079-4087.

Miller, S. G., Carnell, L. and Moore, H. H. (1992). Post-golgi membrane traffic: brefeldin A inhibits export from distal golgi compartments to the cell surface but not recycling. *J. Cell Biol.* **118**, 267-283.

Mundigl, O., Ochoa, G. C., David, C., Slepnev, V. I., Kabanov, A. and De Camilli, P. (1998). Amphiphysin I antisense oligonucleotides inhibit neurite outgrowth in cultured hippocampal neurons. *J. Neurosci.* **18**, 93-103.

Parton, R. G., Simons, K. and Dotti, C. G. (1992). Axonal and dendritic endocytic pathways in cultured neurons. *J. Cell Biol.* **119**, 123-137.

Pfenninger, K. H. and Maylie-Pfenninger, M. F. (1981). Lectin labeling of sprouting neurons. II. relative movement and appearance of glycoconjugates during plasmalemmal expansion. *J. Cell Biol.* **89**, 547-559.

Pravettoni, E., Bacci, A., Coco, S., Forbicini, P., Matteoli, M. and Verderio, C. (2000). Different localizations and functions of L-type and N-type calcium channels during development of hippocampal neurons. *Dev. Biol.* **227**, 581-594.

Reece, J. C., Vardaxis, N. J., Marshall, J. A., Crowe, S. M. and Cameron, P. U. (2001). Uptake of HIV and latex particles by fresh and cultured dendritic cells and monocytes. *Immunol. Cell Biol.* **79**, 255-263.

Rejman, J., Oberle, V., Zuhorn, I. S. and Hoekstra, D. (2004). Size-dependent internalization of particles via the pathways of clathrin- and caveolae-mediated endocytosis. *Biochem. J.* **377**, 159-169.

Ruchhoeft, M. L., Ohnuma, S., McNeill, L., Holt, C. E. and Harris, W. A. (1999). The neuronal architecture of xenopus retinal ganglion cells is sculpted by rho-family GTPases in vivo. *J. Neurosci.* **19**, 8454-8463.

Schaefer, A. W., Kabir, N. and Forscher, P. (2002). Filopodia and actin arcs guide the assembly and transport of two populations of microtubules with unique dynamic parameters in neuronal growth cones. *J. Cell Biol.* **158**, 139-152.

Schnatwinkel, C., Christoforidis, S., Lindsay, M. R., Uttenweiler-Joseph, S., Wilm, M., Parton, R. G. and Zerial, M. (2004). The Rab5 effector rabankyrin-5 regulates and coordinates different endocytic mechanisms. *PLoS Biol.* **2**, E261.

Shao, Y., Akmentin, W., Toledo-Aral, J. J., Rosenbaum, J., Valdez, G., Cabot, J. B., Hilbush, B. S. and Halegoua, S. (2002). Pincher, a pinocytic chaperone for nerve growth factor/TrkA signaling endosomes. *J. Cell Biol.* **157**, 679-691.

Shi, S. H., Jan, L. Y. and Jan, Y. N. (2003). Hippocampal neuronal polarity specified by spatially localized mPar3/mPar6 and PI 3-kinase activity. *Cell* **112**, 63-75.

Sinclair, G. I., Baas, P. W. and Heidemann, S. R. (1988). Role of microtubules in the cytoplasmic compartmentation of neurons. II. Endocytosis in the growth cone and neurite shaft. *Brain Res.* **450**, 60-68.

Swanson, J. A. and Watts, C. (1995). Macropinocytosis. *Trends Cell Biol.* **5**, 424-428.

Symons, M. and Rusk, N. (2003). Control of vesicular trafficking by rho GTPases. *Curr. Biol.* **13,** R409-R418.

Torgersen, M. L., Skretting, G., van Deurs, B. and Sandvig, K. (2001). Internalization of cholera toxin by different endocytic mechanisms. *J. Cell. Sci.* **114**, 3737-3747.

Torre, E., McNiven, M. A. and Urrutia, R. (1994). Dynamin 1 antisense oligonucleotide treatment prevents neurite formation in cultured hippocampal neurons. *J. Biol. Chem.* **269**, 32411-32417.

Tsui, H. C., Ris, H. and Klein, W. L. (1983). Ultrastructural networks in growth cones and neurites of cultured central nervous system neurons. *Proc. Natl. Acad. Sci. USA* **80**, 5779-5783.

Valdez, G., Akmentin, W., Philippidou, P., Kuruvilla, R., Ginty, D. D. and Halegoua, S. (2005). Pincher-mediated macroendocytosis underlies retrograde signaling by neurotrophin receptors. *J. Neurosci.* **25**, 5236-5247.

Valdez, G., Philippidou, P., Rosenbaum, J., Akmentin, W., Shao, Y. and Halegoua, S. (2007). Trk-signaling endosomes are generated by rac-dependent macroendocytosis. *Proc. Natl. Acad. Sci. USA* **104**, 12270-12275.

van Horck, F. P., Weinl, C. and Holt, C. E. (2004). Retinal axon guidance: novel mechanisms for steering. *Curr. Opin. Neurobiol.* **14**, 61-66.

Verhage, M., Maia, A. S., Plomp, J. J., Brussaard, A. B., Heeroma, J. H., Vermeer, H., Toonen, R. F., Hammer, R. E., van den Berg, T. K., Missler, M. et al. (2000). Synaptic assembly of the brain in the absence of neurotransmitter secretion. *Science* **287**, 864-869.

Vogt, L., Giger, R. J., Ziegler, U., Kunz, B., Buchstaller, A., Hermens, W. T. J. M. C., Kaplitt, M. G., Rosenfeld, M. R., Pfaff, D. W., Verhaagen, J. et al. (1996). Continuous renewal of the axonal pathway sensor apparatus by insertion of new sensor molecules into the growth cone membrane. *Curr. Biol.* **6**, 1153-1158.

von Bartheld, C. S. (2004). Axonal transport and neuronal transcytosis of trophic factors, tracers, and pathogens. *J. Neurobiol.* **58**, 295-314.

Watarai, M., Derre, I., Kirby, J., Growney, J. D., Dietrich, W. F. and Isberg, R. R. (2001). Legionella pneumophila is internalized by a macropinocytotic uptake pathway controlled by the Dot/Icm system and the mouse Lgn1 locus. *J. Exp. Med.* **194**, 1081-1096.

Woo, S. and Gomez, T. M. (2006). Rac1 and RhoA promote neurite outgrowth through formation and stabilization of growth cone point contacts. *J. Neurosci.* **26**, 1418-1428.

Yamada, K. M., Spooner, B. S. and Wessells, N. K. (1971). Ultrastructure and function of growth cones and axons of cultured nerve cells. *J. Cell Biol.* **49**, 614-635.

Yamazaki, T., Selkoe, D. J. and Koo, E. H. (1995). Trafficking of cell surface beta-amyloid precursor protein: retrograde and transcytotic transport in cultured neurons. *J. Cell Biol.* **129**, 431-442.

Zakharenko, S. and Popov, S. (2000). Plasma membrane recycling and flow in growing neurites. *Neuroscience* **97**, 185-194.

Zentilin, L., Marcello, A. and Giacca, M. (2001). Involvement of cellular double-stranded DNA break binding proteins in processing of the recombinant adeno-associated virus genome. *J. Virol.* **75**, 12279-12287.